Proceedings World Geothermal Congress 2026
Calgary, Canada, June 8 – 11, 2026

Reservoir Modeling and Long-Term Predictions for the Hofsstadir Geothermal Field, W-Iceland

khishigdelger@iag.ac.mn Khishigdelger Ulziisaikhan[1]*, Gunnar Gunnarsson[2], and Gudni Axelsson[3]
The Institute of Astronomy and Geophysics of Mongolian Academy of Sciences[1]*, Reykjavík Energy[2], GRÓ - GTP[3]

Keywords: Reservoir modeling, Low-temperature reservoir, Regression analysis, Lumpfit modelling

ABSTRACT

This study presents a comprehensive analysis of reservoir modeling for the Hofsstadir geothermal field in W-Iceland, using data collected from 2000 to 2023. The modeling approach involves iterative steps, transitioning from initial data-driven simulations of regression models to more physically explainable lumped parameter models. The comparison of distinct modeling methods, considering different production scenarios, highlights the importance of accurate measurements and effective conceptualization of geothermal fields. A traditional lumped parameter modeling scheme was improved to enable treating production and injection separately, allowing for greater flexibility in incorporating monitoring data. Both the traditional and improved lumped parameter modeling emphasize the closed nature of the system, but sustainable production can be achieved with reinjection. Additionally, predictions for water level and temperature were made up to the year 2040, providing insights into the field's long-term behavior. The knowledge gained from modeling the low-temperature field of Hofsstadir is considered invaluable for the development of similar low-temperature geothermal fields. The study underscores the significance of direct measurements, data validation, and the continuous evolution of modeling techniques for robust geothermal reservoir assessments and sustainable energy development.

1 INTRODUCTION

Reservoirs that have temperature less than 150°C at 1 km depth are considered low temperature in Iceland (Arnórsson, 1995). These low temperature liquid-dominated convective systems' heat sources are hot crust or old volcanic zones, and main flow conductors are faults, fractures, and dykes in the system. Temperature induced density difference drive a convective flow. The main recharge is from groundwater flow from highlands to lowlands. The cold water sinks through open fractures, is heated up by the hot adjacent rock, and then ascends due to decreased density (Bödvarsson, 1983).

The Hofsstadir geothermal field is one of several low-temperature geothermal fields in western Iceland. It supplies district heating to the 1,400 people living in the town of Stykkishólmur, which is located 5 km northwest of the field. The field has been in continuous operation since the end of 1999, without any significant issues considering its closed boundary nature. This long-standing success makes it a classic example of sustainable production and successful reinjection. In this study, we simulate various production scenarios, estimate the sustainability of the system, and gain a deeper understanding of it through regression modelling and lumped parameter modelling.

The Hofsstadir geothermal system was discovered during extensive regional surveys in northern Snaefellsnes Peninsula, Western Iceland, involving the drilling of approximately 120 shallow exploration wells in 1995. The high mineral content of the water has led to its utilization for balneological and psoriasis treatment purposes. The geothermometric equations suggest that reservoir temperature is around 90°C. Isotopic ratios for δD and δ18O suggest that the hot water in the Hofsstadir field originates from the latest glacial period, pre-Holocene, consistent with its classification as 'mature' water based on chemistry. Furthermore, the elevated calcium concentration in the water implies a long-term equilibrium with the rock matrix, which in turn suggests a closed system (Kristmannsdóttir et al., 2005).

Analysis of the well temperature gradients revealed a distinctive NW-SE direction anomaly of 400°C/km (Guo, 2008), in contrast to the regional temperature gradient of 70°C/km (Olafsson et al., 2004 in Axelsson et al., 2005). In 1996, the production well HO-01 was drilled to a depth of 855 meters at the heart of the highest temperature anomaly (fissure) shown in Figure 1. The well intercepted two primary feed zones with water temperatures ranging from 86°C to 88°C (Guo, 2008) and was cased down to a depth of 156 meters. The first feed zone, located at a depth of 171-175 meters within a basaltic layer, contributes 7% of the total flowrate. In contrast, the second feed zone is situated at a depth of 819 meters and is attributed to fractures in a gabbroic intrusion, accounting for 90% of the total flowrate.

At the end of the drilling, an air-lift test was conducted and concluded that the well's productivity was good, with a flowrate of 40 L/s. Afterward, a five-month test was conducted with a pumping flowrate of 15-20 L/s to assess the feasibility of constructing a district heating system and infrastructure for the town of Stykkishólmur. The conclusion, as reported by Björnsson et al. (1997), indicated that the project was feasible. However, due to the high salinity of the geothermal water in the field (Cl-Ca-Na type), the heating system was designed to include a central heat exchanger that utilizes closed water circulation (Kristmannsdóttir et al., 2005).

Starting from late 1999, well HO-01 has been used as a production well with an average flowrate of 25 L/s. Since the beginning, its pressure and temperature have been continuously monitored. However, despite maintaining a relatively constant production level, except for seasonal fluctuations, production well HO-01 experienced continuously increasing water level drawdown. In response to this issue, injection well HO-02 was drilled in 2006 and commenced injecting water back into the system in April 2007. It was drilled down to the depth of 413.2 meters 1200 meters north of production well HO-01, into another hot fissure, with the primary feed zone situated at a depth of 319 meters. Shortly after the injection commenced, the water level drawdown in the production well decreased significantly, with no substantial evidence of cooling. Therefore, the injection was successful and has been continuing for several decades until now.

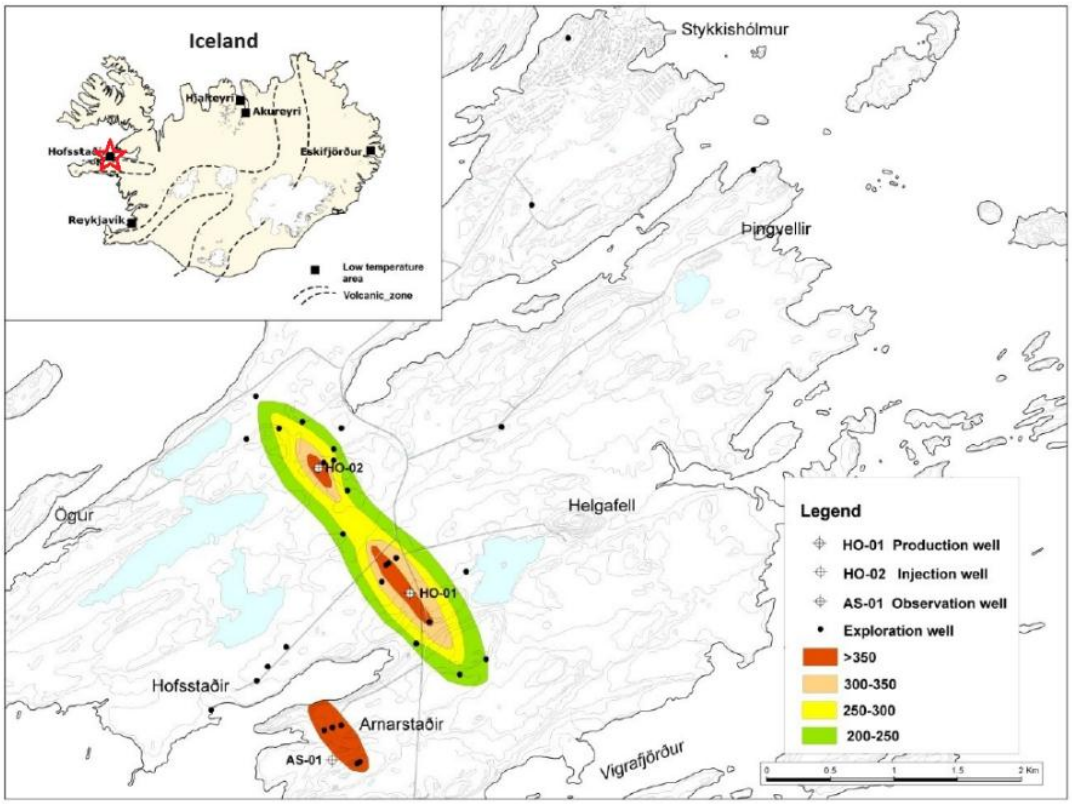


Figure 1. The map of temperature gradient of Hoffstadir geothermal field and Stykkishólmur town (modified from Guo, 2008)

2 METHODS

In this work the modelling process of the Hofsstadir field has been evolved through a series of step-by-step improvements. Initially, a model was created using only historical data on production, injection, and measured water levels, without incorporating any physical properties of the field nor any physical constrains. This model was developed to simulate the system and make predictions for constant production levels, consistent with the current state, as well as for increasing production by 2% annually. Subsequently, a lumped parameter model was employed, utilizing the LUMPFIT program from the ICEBOX package to fit the model and develop it with the same prediction scenarios. Finally, an improved conceptual framework of the field was used to create a new lumped parameter model. This model was developed with straightforward calculations using Python, offering a more refined approach compared to the earlier models.

2.1 Regression model

The regression model relies exclusively on historical data of production, injection, and water levels recorded during the production history. It does not incorporate any reservoir physical properties such as size, porosity, permeability, or compressibility, nor any other physical constrains. This method proves particularly valuable when these properties are not well-known or when quick predictions are required for expedited decision-making processes.

The primary concept of this model involves predicting current water levels by identifying the constants in the linear relationships between water levels, production rates, and injection rates from previous time steps. The model uses monthly average values for each recorded parameter. In other words, the model operates on a monthly time steps, requiring interpolation of all measurements to monthly intervals.

Mathematical representation of the pressure model is illustrated in equation (1), where the water level h_i is calculated from previous values of the water level, and current and previous production and injection rate values, Qp_i and Qi_i respectively.

$$h_i = d + \sum_{n=0}^{N_1} a_n Qp_{i-n} + \sum_{n=0}^{N_2} b_n Qi_{i-n} + \sum_{n=1}^{N_3} c_n h_{i-n} \tag{1}$$

where h = Water level [m];
Q_p = Production rate [L/s];
Q_i = Injection rate [L/s];
a_n, b_n, c_n, and d are constants.

To assess the stability of the model, three different scenarios have been calculated: one scenario with N = N_1 = N_2 = N_3 = 3, another with N = N_1 = N_2 = N_3 = 5, and a third with N = N_1 = N_2 = N_3 = 6. In equation (2), a matrix representation for the N = 3 scenario of water level calculation in equation (1) is shown.

$$\overbrace{\begin{bmatrix} Qp_{i-3} & Qp_{i-2} & Qp_{i-1} & Qp_i & Qi_{i-3} & Qi_{i-2} & Qi_{i-1} & Qi_i & h_{i-3} & h_{i-2} & h_{i-1} & 1 \\ Qp_{i-2} & Qp_{i-1} & Qp_i & Qp_{i+1} & Qi_{i-2} & Qi_{i-1} & Qi_i & Qi_{i+1} & h_{i-2} & h_{i-1} & h_i & 1 \\ Qp_{i-1} & Qp_i & Qp_{i+1} & Qp_{i+2} & Qi_{i-1} & Qi_i & Qi_{i+1} & Qi_{i+2} & h_{i-1} & h_i & h_{i+1} & 1 \\ \vdots & \vdots & \vdots & \vdots & \vdots & \vdots & \vdots & \vdots & \vdots & \vdots & \vdots & \vdots \\ Qp_{i+n-3} & Qp_{i+n-2} & Qp_{i+n-1} & Qp_{i+n} & Qi_{i+n-3} & Qi_{i+n-2} & Qi_{i+n-1} & Qi_{i+n} & h_{i+n-3} & h_{i+n-2} & h_{i+n-1} & 1 \end{bmatrix}}^{\mathrm{P}} \times \underbrace{\begin{bmatrix} a_0 \\ a_1 \\ a_2 \\ a_3 \\ b_0 \\ b_1 \\ b_2 \\ b_3 \\ c_1 \\ c_2 \\ c_3 \\ d \end{bmatrix}}_{\mathrm{C}} = \underbrace{\begin{bmatrix} h_i \\ h_{i+1} \\ h_{i+2} \\ \vdots \\ h_{i+n} \end{bmatrix}}_{\mathrm{W}} \tag{2}$$

To simplify the linear equation (2), we represent the parameter part as 'P', the constant part as 'C', and the water level part as 'W'. Multiplying the measured water level part (W) by the transpose and inverse of the parameters (P) provides the constants (C) used for future water level predictions as shown by equation (3).

$$\begin{aligned} P \times C = W \quad &\Leftrightarrow \quad P^T P \times C = P^T \times W \\ \Leftrightarrow (P^T P)^{-1} \times (P^T P) \times C &= (P^T P)^{-1} \times P^T \times W \\ \Leftrightarrow C &= (P^T P)^{-1} \times P^T \times W \end{aligned} \tag{3}$$

The same method is applied to temperature prediction. The current production temperature is considered dependent on previous measured production and injection temperatures, as well as production and injection rates as shown in equation (4). Since injection temperature data is available from 2010, the model is developed using measured values of all parameters from that date onwards. For prediction purposes, the injection temperature is assumed to be constant at 40°C.

$$Tp_i = e + \sum_{n=0}^{N_1} a_n Qp_{i-n} + \sum_{n=0}^{N_2} b_n Qi_{i-n} + \sum_{n=0}^{N_3} c_n Ti_{i-n} + \sum_{n=1}^{N_4} d_n Tp_{i-n} \tag{4}$$

where T_p = Production temperature [°C];
T_i = Injection temperature [°C];

Q_p = Production rate [L/s];
Q_i = Injection rate [L/s];
a_n, b_n, c_n, d_n, and e are constants.

2.2 Lumpfit modelling of the Hofsstadir field

The lumped parameter model, executed through the LUMPFIT program, automatically fits analytical response functions of the model to observed data by computing model parameters using a non-linear iterative least-squares method. This model is comprised of tanks and resistors (conductors) connecting them, as illustrated in Figure 2. Since the system is analogy to electric series circuit, for further simple explanation, this model will be named as lumpfit series model in this report.

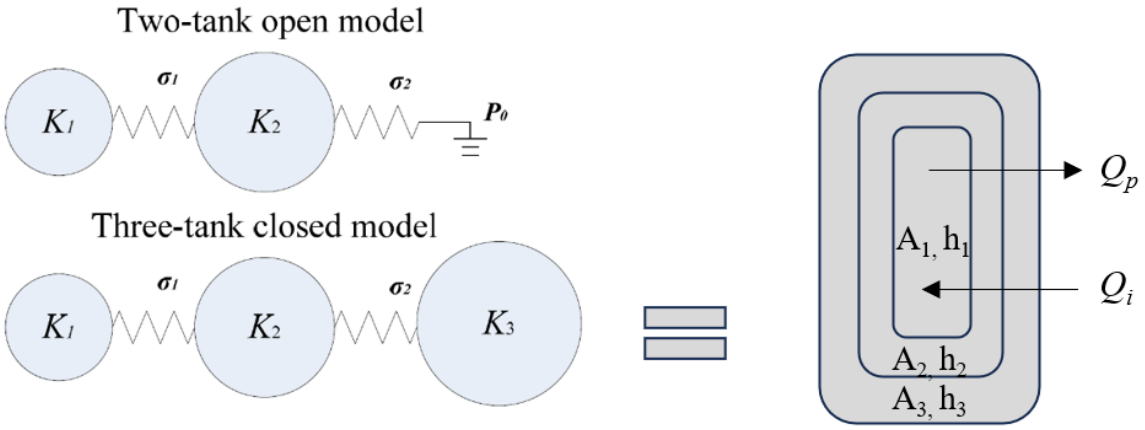


Figure 2. Lumpfit series model scheme (Axelsson, 1989) with easier illustration of three tank closed system

The time dependent pressure response of open model with N tank and constant production Q is given by equation (5). For closed model, the time dependent pressure response is shown by equation (6), where A_i^*, L_i, B are coefficients of functions of storage (κ_i) and conductance of resistors (σ_i).

$$\Delta P(t) = -\sum_{i=1}^{N} Q \frac{A_i^*}{L_i}[1 - e^{it}] \qquad (5)$$

$$\Delta P(t) = -\sum_{i=1}^{N-1} Q \frac{A_i^*}{L_i}[1 - e^{-L_i t}] - QBt \qquad (6)$$

In the case of the lumpfit series model, it treats production and injection sites as if they are within the same tank. In other words, it doesn't differentiate between production and injection by specifying their amounts and locations separately. Instead, it takes the net flow (production - injection) of the system as input. The lumpfit series is calculated by ICEBOX package from ISOR. The program fits the modelled parameters to the measured data, which is water level and production. Following reservoir properties were selected for program execution. The reservoir temperature was chosen as 87°C, the thickness was assumed to be 1000 meters, porosity was set at 10% (a commonly used rule of thumb in Iceland), water density was established at 970 kg/m^3, and the rock compressibility was chosen as 3e-11 1/Pa.

However, given that the distance between the two wells is approximately 1200 meters, the assumption of the same production and injection site diverges from reality. To account for this distance between production well HO-01 and injection well HO-02, various scenarios were simulated and compared. These scenarios are based on the portion of the injection that affects the water level in the production well HO-01. Three different scenarios were compared, in which 80%, 90%, and 100% of the injection rate contribute to the water level in the HO-01 production well.

2.3 Lumpfit model with better conceptual scenario

As mentioned earlier, the previous model assumed that the system was both producing and injecting from the same location, which is unlikely given the substantial distance between the wells. To address this, the concept was developed for another LUMPFIT model that considers production and injection occurring from two distinct tanks. This adjustment was made to enhance the quality of the fitting and involved the use of simple linear equations within a daily time-step numerical approach. As depicted in Figure 3, this version of lumpfit is analogy to electric parallel circuit, therefore, for future convenience to distinguish from the traditional lumpfit model (series), it will be named *lumpfit parallel*.

In this model, the water level of the production well HO-01 is considered as the water level of tank 1, while the water level of the injection well HO-02 is considered as the water level of tank 2. The two-tank model only takes into account two tanks, each having the production and injection wells. In contrast, the three-tank model introduces a larger tank surrounding the two existing tanks. This larger tank is connected to the environment, and all three tanks are interconnected. Notably, when the third tank was not connected to the environment, it had a significant impact on the results. Consequently, a fourth tank that is entirely closed off from the environment was added around the third tank as depicted in Figure 3 to test if it would yield better results, considering that the reservoir has been treated as a closed boundary system.

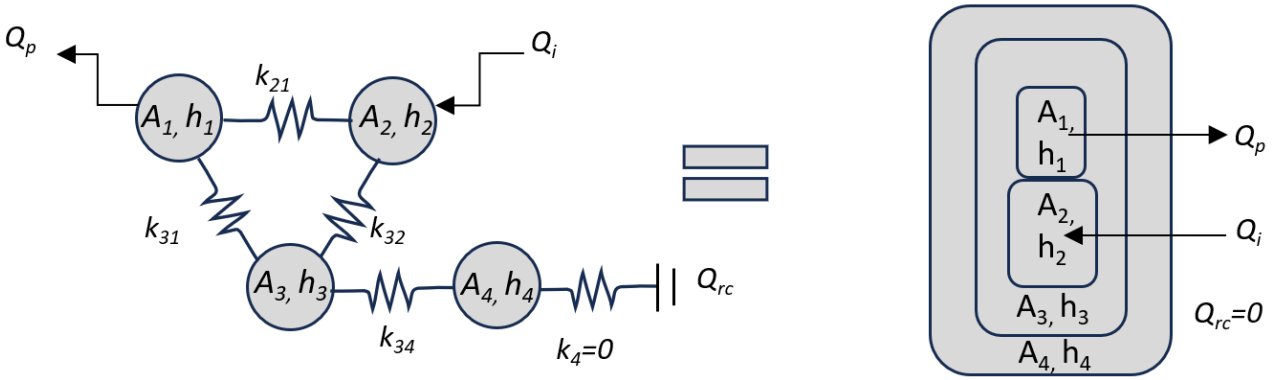


Figure 3. Lumped parallel model format with easier illustration representing better conceptual model of 4-tank closed system. Here A represents surface area and h represents water level.

The flow from one tank to another is defined by equation (7). The water levels are calculated using the flow rates, permeabilities from one tank to another, surface area, and porosity of each tank as it is illustrated in equation (8).

$$Q_{21} = (h_2 - h_1)k_{21} \qquad Q_{32} = (h_3 - h_2)k_{32} \qquad Q_{31} = (h_3 - h_1)k_{31}$$
$$Q_{34} = (h_3 - h_4)k_{34} \qquad Q_{rc} = (h - h_4)k_4 \tag{7}$$

$$\Delta h_1 = \frac{Q_{21}+Q_{31}-Q_p}{A_1\phi}\,\Delta t \qquad \Delta h_2 = \frac{Q_{32}-Q_{21}+Q_i}{A_3\phi}\,\Delta t$$
$$\Delta h_3 = \frac{Q_{43}-Q_{31}-Q_{32}}{A_3\phi}\,\Delta t \qquad \Delta h_4 = \frac{Q_{rc}-Q_{43}}{A_4\phi}\,\Delta t \tag{8}$$

where Q_{nm} = Flow from n^{th} to m^{th} tank [L/s];
Q_{rc} = Recharge flow rate [L/s];
h_n = Water level in n^{th} tank [m];
h = Water level of environment [m];
A_n = Surface area of n^{th} tank [m^2];
k_{nm} = Permeability between n^{th} to m^{th} tank [m^2/s];
ϕ = Porosity [%];
Δt = Time step/a day [s].

Given that the exact values of surface areas and permeabilities between each tank are not known, these parameters are determined through an iterative inverse process. The values are adjusted by computing the difference between the measured water level and the calculated water level until a satisfactory fitting is achieved. However, it's worth noting that the water level of the injection well was lower than that of the production well. While this might suggest water flow from production to injection, the reality is different. The lower water level in the injection well is likely due to density differences resulting from temperature variations in each well, shifting the water levels.

To use these water levels as legitimate representations of pressure when assessing the fitting of the calculated pressure in the model, an adjustment is made to the water level of tank 2 during the iteration process when other parameter values are selected. Table 3 provides the best-fitting areas, permeabilities between tanks, and second tank water level shift values and errors (S_2) using equation (15), which are calculated by adding the square of the difference between the measured and calculated water levels of the two tanks, explained in result

section. It's important to note that the fitting process does not include measurements of the water levels in the third and fourth tanks.

3 RESULTS

The three different reservoir modelling approaches were tested and utilized for Hofsstadir geothermal field. In this chapter, the comparison between them will be discussed.

Firstly, the results of the regression model are presented numerically in Table 1, and the predicted values for October 2040 after 17 years of usage for two production scenarios are provided in Table 2. In case of the temperature, the first scenario maintains constant production and injection rates in Figure 4, while the second scenario involves 2% annual increases in both production and injection in Figure 5. Then, in terms of water level, all three models are compared together in each prediction scenario as shown in Figure 6 and Figure 7. To select the best fitting model, an error equation is used to compare models. The general equation of error is presented by equation (9).

$$S_1 = \sum\left(\frac{v_{measured} - v_{modeled}}{\sigma}\right)^2 \quad (9)$$

where S_1 = Error;
$v_{measured}$ = Measured value;
$v_{modeled}$ = Modeled value;
σ = Accuracy of the measurement.

In case of water level measurements, the accuracy is chosen as 0.1 m, while for temperature measurements it is chosen as 1°C.

In Table 1, 'calculated error' represents the error when computing the next time-step parameter using the previously calculated value, while 'measured error' reflects the error when using the real measured value to calculate next time step value to the equations (1) and (4). In other words, calculated and measured errors differ how the modelled values are calculated. The measured error is significantly smaller because it doesn't accumulate errors over time. Therefore, the best-fitting model among the three regression models tested is the 6-time step model (N=6), as defined in equation (1).

Table 1. HO-01 well water level fitting errors responding when using calculated values and measured values of water level as input to regression model

Model, water level	Calculated error	Measured error	Model, temperature	Calculated error	Measured error
3-time step	1903.84	1.46	3-time step	10431.26	1154.42
5-time step	8771.63	1.32	5-time step	9532.24	1077.72
6-time step	710.84	1.24	6-time step	8239.39	1057.79

Table 2. Predictions of HO-01 well water level and temperature by regression model as of October 2040

Model, water level	Prediction 1, m	Prediction 2, m	Model, temperature	Prediction 1, °C	Prediction 2, °C
3-time step	-25.01	-40.57	3-time step	84.54	84.07
5-time step	-24.91	-43.78	5-time step	84.44	82.54
6-time step	-24.55	-42.80	6-time step	84.38	84.29

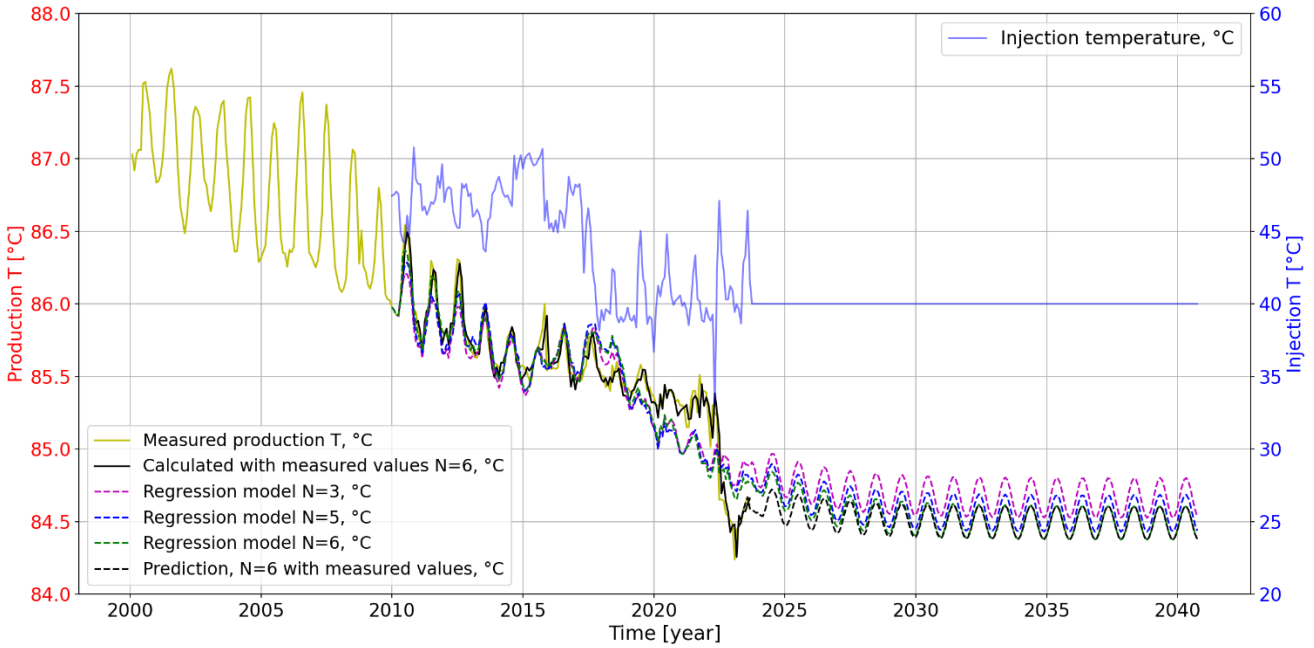


Figure 4. Regression model temperature prediction 1 scenario with N = 3, 5, and 6

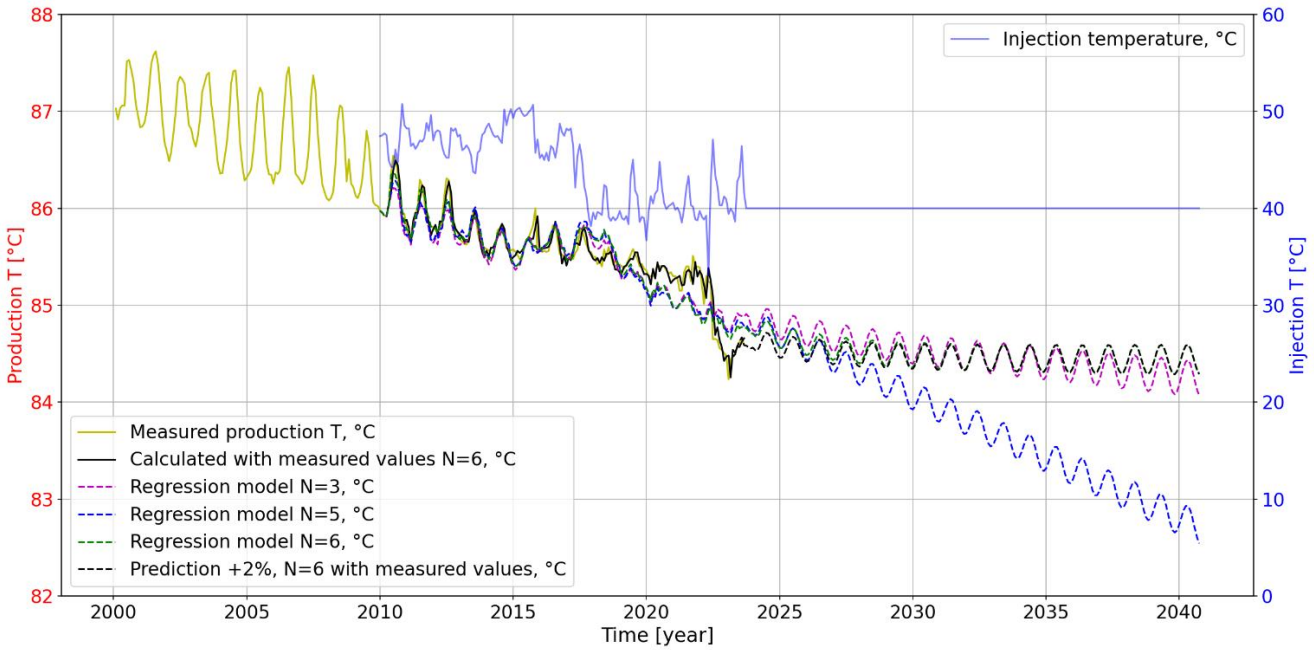


Figure 5. Regression model temperature prediction 2 scenario with N = 3, 5, and 6

Secondly, the results of the lumpfit series model are presented in Table 3. Based on the standard deviation values, the model that best fits the data is the one where the entire flow (100%) of the injection is considered, i.e., subtracted from the flow from the production well. Additionally, when comparing the 2-tank open and 3-tank closed models, the 3-tank closed model closely aligns with the measured water level values from HO-01 well. The prediction scenarios are same as that of regression model. The first prediction scenario is keeping the current rates as it is for 17 years. The second prediction scenario is increasing production and injection rates 2% annually for 17 years until October of 2040 as both depicted as black lines in Figure 6 and Figure 7.

Table 3. HO-01 well water level fitting error and predictions of two tanks open and three tanks closed by lumpfit series model as of October 2040

Model, water level	Standard deviation, bar-g		Prediction 1, m		Prediction 2, m	
	2 open	3 closed	2 open	3 closed	2 open	3 closed

100% injection	4.33	4.16	-23.62	-28.57	-31.76	-36.67
90% injection	5.16	5.17	-21.20	-21.20	-28.89	-28.89
80% injection	7.72	7.73	-19.31	-19.31	-26.51	-26.51

Third, lumpfit parallel model results are shown in Table 4. The best fitting model is the 4-tank closed model according to the lowest error value calculated by equation (10).

$$S_2 = \sum(v_{measured} - v_{modeled})^2 \quad (10)$$

To compare all the models, prediction scenarios are same as previous two models ´.

Table 4. HO-01 well water level fitting error and predictions of tank 1 and tank 2 by lumpfit parallel model as of October 2040

Model, water level	Error, m^2	Prediction 1, m		Prediction 2, m	
		Tank 1	Tank 2	Tank 1	Tank 2
2-tank	325465.31	-32.45	-19.35	-42.91	-25.31
3-tank	160647.69	-23.85	-20.75	-31.06	-26.88
4-tank	148200.91	-30.02	-23.75	-37.15	-28.71

When comparing the best-fitting models from each category for their prediction results, in the case of the first scenario, illustrated in Figure 6, the most pessimistic prediction arises from the calculated 4-tank lumped parallel model, with a water level value of -30.02 m as of October 2040. Conversely, the most optimistic forecast is produced by the regression model yielding a value of -24.55 m, using 6-time steps. Falling between these extremes is the lumpfit series model, which assumes 3 tanks closed and 100% injection subtracted from the production rate, resulting in a prediction of -28.57 m as of October 2040.

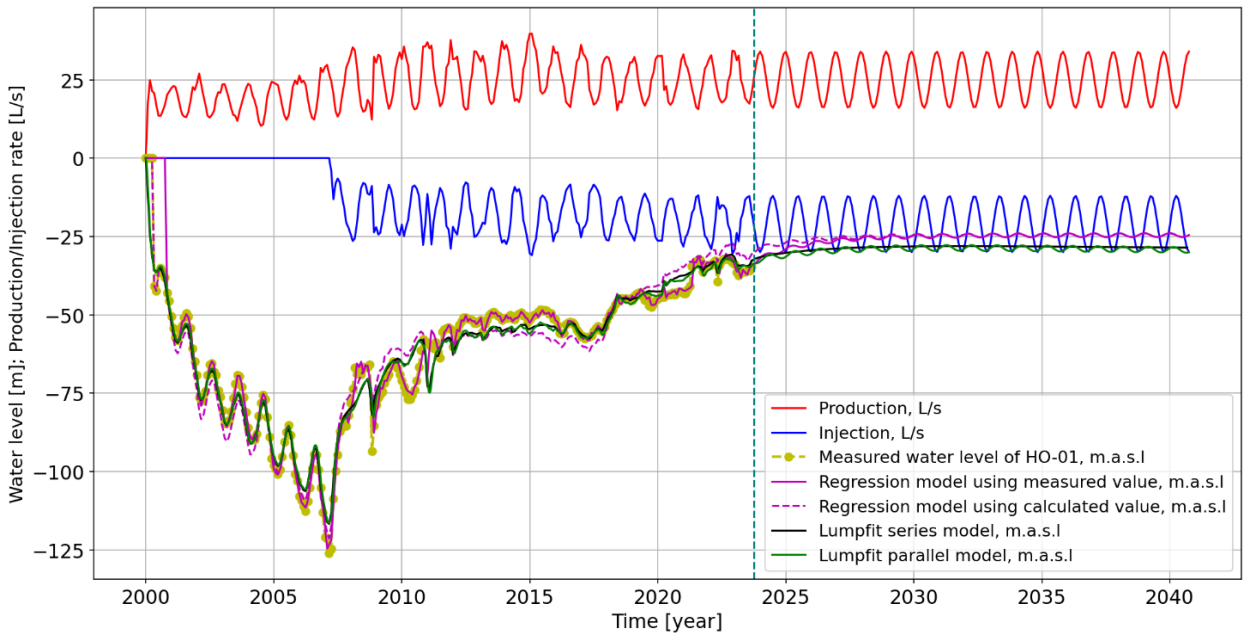


Figure 6. Best fitting models from each method are compared together for first prediction scenario, which is starting from dashed line representing year 2023

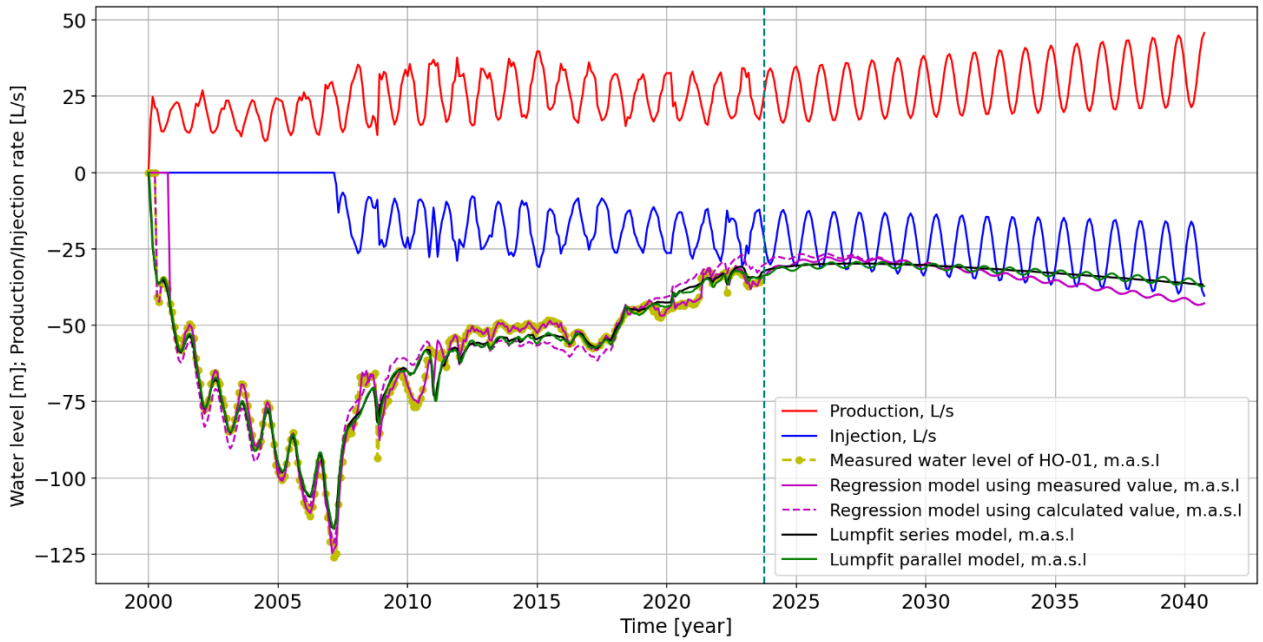


Figure 7. Best fitting models from each method are compared together for second prediction scenario, which is starting from dashed line representing year 2023

For the second prediction scenario shown in Figure 7, the most pessimistic prediction comes from the regression model using 6-time steps at -42.8 m, while the most optimistic forecast is -36.67 m from the 3-tank closed system of lumpfit series model. In between, the 4 tanks closed (from lumpfit parallel) system result is -37.15 m. However, the general trend indicates that the 3 tanks closed (from lumpfit series) model behaves as an average of the 4-tank closed model while it is fluctuating over 3 tanks closed model result.

The size of the reservoir from the fitting of lumped parameter models are presented in Table 5.

Table 5. Comparison of areas resulted from lumpfit series and lumpfit parallel models

Area	Lumpfit series		Lumpfit parallel	
	3T Closed/unconfined	3T Open/confined	3T Open	4T Closed
A_1 [km^2]	0.031	4.471	0.010	0.004
A_2 [km^2]	0.198	28	0.014	0.019
A_3 [km^2]	16	2368	0.2	0.194
A_4 [km^2]				13

In Table 5, total of A_1 and A_2 of the lumpfit series 3-tank closed unconfined model is very similar to the total of A_1, A_2, and A_3 of 3 tanks open and 4-tank closed model. In other words, lumpfit series and lumpfit parallel models´ results in terms of the reservoir area are quite consistent with each other.

4 CONCLUSION

The modelling of the Hofsstadir field was undertaken in a series of iterative steps, with each step aimed at enhancing the accuracy and predictive capabilities of the models. These steps have ranged from initial data-driven simulations to more physically explainable lumped parameter models, all designed to gain a deeper understanding of the field's behaviour and reservoir characteristics.

Each category of models is simulated with slightly different scenarios to achieve the most optimal parameters within their respective model types. Once these distinct models are fine-tuned, they are compared with one another in terms of their fitting to the measured values and prediction performance. Two prediction scenarios were studied. The first one is just keeping the current production and injection rates constant until October 2040, i.e., for 17 years. The second scenario assumes a 2% annual increase in production and injection rates over the same period. The final water level predicted for the first scenario ranges from -24.55 m to -30.02 m, and for the second scenario, ranges from -36.67 m to -42.80 m across all models. The temperature prediction from the

regression model for the first scenario ranges from 84.38°C to 84.54°C almost same as the current temperature, whereas for the second scenario it ranges from 82.54°C to 84.29°C, cooling around 2°C from current temperature. This small change could be realistic despite some divergence between different number of time step models, since the water temperature has only cooled down by 2.5°C for over 20 years. The reason could be highly related to reinjection into another hot fissure of the system.

The regression modelling aligns almost perfectly with the measured values; however, for predictions, there are no physical constraints, and the accuracy of measurements plays a crucial role in the model's outcomes. Inaccuracies in measurements can significantly impact future predictions. Additionally, the choice of the number of time steps in the calculation can have a substantial effect on the results, as illustrated in the temperature prediction in Figure 5 when production and injection rates are increasing. Further studies could explore the optimal number of time steps and assess the influence of each parameter on the results. Despite this, with accurate measurements and a gradual change in production and injection rates, the predictions can be reliable, making the model more suitable for short-term prognosis.

Traditional lumpfit modelling, defined as lumpfit series in this report, is convenient, fast, reflects some physical properties of the reservoir, and could be reliable for long-term prognosis. However, it lacks flexibility in distinguishing production and injection locations. Given the thermal gradient map of the Hofsstadir field in Figure 1, where injection and production locations are separated by 1200 m and situated on distinct hot fissures, it was reasonable to explore a conceptual setting that distinguishes production and injection into two separate tanks.

The development of the lumpfit parallel model, where production and injection can be assigned to different tanks, has the potential to offer more accurate results, as it takes the geological setting and the location of injection and production wells better into account. Moreover, the governing equation is straightforward, and it is possible to add tanks and wells in a flexible manner for production, injection, and monitoring. This allows to use water level data from more than one well.

In general, all the models showed that keeping the current average level of production rate, which is around 25 L/s fluctuating from 16 L/s in summer to 34 L/s in winter, and injection rate, which is around 21 L/s fluctuating from 12 L/s in summer to 30 L/s in winter could result in equilibrium of the system after 5 years from now as shown in Figure 6.

The area of tank 1 of lumpfit series model should be close or similar to the combined area of tank 1 and tank 2 of lumpfit parallel model according to the conceptual settings of the two models shown in Figure 2 and Figure 3. This was the case as can be seen on the results shown in Table 5. Additionally, tank 2 of the lumpfit series model and tank 3 of the lumpfit parallel model are nearly identical, also aligning with the conceptual framework. Furthermore, the closed nature of the system has been confirmed by good fitting results from closed models, specifically the 3-tank closed model for the lumpfit series and the 4-tank closed model for the lumpfit parallel.

Moreover, it is noteworthy that the time steps are different for all the models. In case of the regression model the values of each parameter are down sampled to monthly values, while for lumpfit parallel model, parameters are up sampled to daily values for stability. Then for lumpfit series modelling, data or parameters are used as they are measured.

Acknowledgements

I would like to express my gratitude for Dr. Gudni Axelsson, Mrs. Málfrídur Ómarsdóttir, and Mr. Ingimar G. Haraldsson for giving me the opportunity to participate in the training and for their unwavering support throughout our stay in Iceland. My special thanks to my supervisor Gunnar Gunnarsson for his detailed review and invaluable guidance. The data utilized in this study was sourced from the Reykjavík Energy company database.

REFERENCES

Arason, Th., and Björnsson, G.: *ICEBOX*. 2nd edition, Orkustofnun, Reykjavík, (1994), 38 pp.

Arnórsson, S.: Geothermal systems in Iceland: Structure and conceptual models II. Low-temperature areas, *Geothermics,* **24**, (1995), 603-629.

Axelsson, G.: Simulation of pressure response data from geothermal reservoir by lumped parameter models, *Proceedings of the 14th Workshop on Geothermal Reservoir Engineering,* Stanford University, California, 257-263, (1989).

Axelsson, G., Björnsson, G., Egilsson, Th., Flóvenz, Ó.G., Gautason, B., Hauksdóttir, S., Ólafsson, M., Smárason Ó.B., and Saemundsson, K.: Nature and properties of recently discovered hidden low-temperature geothermal reservoirs in Iceland, *Proceedings of the World Geothermal Congress, Antalya, Turkey,* CD, (2005), 10 pp.

Björnsson, G., Axelsson, G., Kristmannsdóttir, H., Saemundsson, K., Thórhallsson, S., and Hardardóttir, V.: Production testing of well HO-01 at Hofsstadir in Helgafell´s county, Orkustofnun, Reykjavík, report OS-97042 (in Icelandic), (1997), 36 pp.

Bödvarsson, G.: Temperature/flow statistics and thermomechanics of low-temperature geothermal systems in Iceland, J. Volc. Geoth. Res, **19**, (1983), 255-280.

Guo, G.: Assessment of the Hofsstadir geothermal field, W-Iceland, by lumped parameter modelling, Monte Carlo simulation and tracer test analysis, Report 18 in: Geothermal Training in Iceland 2008, UNU-GTP, Iceland, (2008), 247-279.

Kristmannsdóttir, H., Sveinbjörnsdóttir, Á.E., and Sturludóttir, Á.: Geochemistry, origin and balneological properties of a geothermal brine at Hofsstadir near Stykkishólmur, Iceland, *Proceedings of the World Geothermal Congress*, Antalya, Turkey, CD, (2005), 5 pp.

Olafsson, M., Saemundsson, K., and Axelsson, G.: The Stykkisholmur hitaveita, W-Iceland, Exploration, construction and first three years of operation, *26th Nordic Geological Winter Meeting*, Uppsala, Sweden, (2004).